Valence-band anticrossing in mismatched III-V semiconductor alloys

K. Alberi,[1,2] J. Wu,[1,2] W. Walukiewicz,[1] K. M. Yu,[1] O. D. Dubon,[1,2] S. P. Watkins,[3] C. X. Wang,[3] X. Liu,[4] Y.-J. Cho,[4] and J. Furdyna[4]

[1]*Materials Sciences Division, Lawrence Berkeley National Laboratory, Berkeley, California 94720, USA*

[2]*Department of Materials Science and Engineering, University of California, Berkeley, California 94720, USA*

[3]*Department of Physics, Simon Fraser University, Burnaby, British Columbia, Canada V5A 1S6*

[4]*Department of Physics, University of Notre Dame, Notre Dame, Indiana 46556, USA*

(Received 26 May 2006; revised manuscript received 15 November 2006; published 16 January 2007)

We show that the band gap bowing trends observed in III-V alloys containing dilute concentrations of Sb or Bi can be explained within the framework of the valence-band anticrossing model. Hybridization of the extended *p*-like states comprising the valence band of the host semiconductor with the close-lying localized *p*-like states of Sb or Bi leads to a nonlinear shift of the valence-band edge and a reduction of the band gap. The two alloys $GaSb_xAs_{1-x}$ and $GaBi_xAs_{1-x}$ are explored in detail, and the results are extrapolated to additional systems.

DOI: 10.1103/PhysRevB.75.045203 PACS number(s): 71.20.Nr, 71.55.Eq, 78.30.Fs

I. INTRODUCTION

Amid the current activity in semiconductor alloy research, materials containing either Bi or Sb have emerged as potential candidates for long wavelength applications. Comparable to III-N-V compounds, recent reports show that the band gap of GaAs redshifts considerably upon the addition of only a few atomic percent of Bi or Sb.[1–9] Furthermore, it has been suggested that $GaBi_xAs_{1-x}$ exhibits other anomalous properties, such as a reduced temperature dependence of the band gap as well as giant spin-orbit splitting.[5,10] However, little is presently known about the exact mechanisms by which these alloying elements influence the properties of III-V compounds. Using $GaSb_xAs_{1-x}$ and $GaBi_xAs_{1-x}$ as exemplary systems, we propose a theoretical model of the electronic structure of III-Sb-V and III-Bi-V alloys based upon that describing other similar dilute semiconductor alloy systems.

The band anticrossing (BAC) model was developed to explain the unusual features of the electronic structure of a class of semiconductors termed highly mismatched alloys (HMAs) and was initially applied to those systems in which highly electronegative isoelectronic impurity atoms are incorporated onto the anion sublattice of a III-V or II-VI compound semiconductor.[11] Well-known examples include GaN_xAs_{1-x} (Ref. 12) and ZnO_xTe_{1-x} (Ref. 13) in which a large-scale bowing of the band gap,[14] an increase of the electron effective mass,[15] and a reduction of the pressure dependence of the band gap[11] have been observed upon the addition of N or O, respectively. In contrast to alloys with mixed cation elements, highly electronegative elements on the anion sublattice introduce localized defect states sufficiently close to the conduction-band edge of the host matrix to undergo a quantum anticrossing interaction with the extended states of the matrix.[16] This interaction produces a splitting of the conduction band into E_- and E_+ levels, with the downward movement of the former leading to the band gap bowing observed in these dilute alloys. The term "mismatched" may also refer to a disparity in the atomic size of the alloying element occupying the anion sublattice. The defect states of large-sized impurities with first ionization energies less than that of the host anion often lie near the valence-band edge of the host semiconductor. Hybridization between the two results in a modification of the valence band in a similar manner to the restructuring of the conduction band. As the atomic diameters of Sb and Bi are the largest of the group V elements, we expect such interactions to occur in $GaSb_xAs_{1-x}$ and $GaBi_xAs_{1-x}$, and these alloys may be considered in the context of the valence-band anticrossing (VBAC) model. Indeed, the explicit restructuring of the valence band that has been experimentally observed in other III-V and II-VI alloy systems, including $GaN_{1-x}As_x$, $ZnSe_{1-x}Te_x$, and ZnS_xTe_{1-x}, has been attributed to such anticrossing interactions.[17,18]

In this paper we consider the effects of the substitution of As atoms by Sb and Bi to form dilute $GaSb_xAs_{1-x}$ and $GaBi_xAs_{1-x}$, respectively, and show that the band gap bowing and increase of the spin-orbit splitting observed in these alloys are well explained by the valence-band anticrossing model (VBAC).

II. VALENCE-BAND ANTICROSSING MODEL

The valence-band structures of As-rich $GaSb_xAs_{1-x}$ and $GaBi_xAs_{1-x}$ alloys were developed within the realm of the $\mathbf{k}\cdot\mathbf{p}$ formalism. In each case, the standard 6×6 Hamiltonian describing the four Γ_8 and two Γ_7 valence bands of GaAs was modified by the addition of the six localized *p*-like states of the minority Sb or Bi atoms with basis functions identical to those describing the host semiconductor.[19] To address the issue of the random placement of impurity atoms in the crystal lattice we have used a previously developed method of configurational averaging carried out within the coherent potential approximation, which has been shown to restore translational symmetry.[11,20] The resulting 12×12 matrix Hamiltonian is given as

$$H_V = \begin{vmatrix}
H & \alpha & \beta & 0 & \frac{i\alpha}{\sqrt{2}} & -i\sqrt{2}\beta & V(x) & 0 & 0 & 0 & 0 & 0 \\
\alpha^* & L & 0 & \beta & \frac{iD}{\sqrt{2}} & i\sqrt{\frac{3}{2}}\alpha & 0 & V(x) & 0 & 0 & 0 & 0 \\
\beta^* & 0 & L & -\alpha & -i\sqrt{\frac{3}{2}}\alpha^* & \frac{iD}{\sqrt{2}} & 0 & 0 & V(x) & 0 & 0 & 0 \\
0 & \beta^* & -\alpha^* & H & -i\sqrt{2}\beta^* & \frac{-i\alpha^*}{\sqrt{2}} & 0 & 0 & 0 & V(x) & 0 & 0 \\
\frac{-i\alpha^*}{\sqrt{2}} & \frac{-iD}{\sqrt{2}} & i\sqrt{\frac{3}{2}}\alpha & i\sqrt{2}\beta & S & 0 & 0 & 0 & 0 & 0 & V(x) & 0 \\
i\sqrt{2}\beta^* & -i\sqrt{\frac{3}{2}}\alpha^* & \frac{-iD}{\sqrt{2}} & \frac{i\alpha}{\sqrt{2}} & 0 & S & 0 & 0 & 0 & 0 & 0 & V(x) \\
V(x) & 0 & 0 & 0 & 0 & 0 & E_{imp} & 0 & 0 & 0 & 0 & 0 \\
0 & V(x) & 0 & 0 & 0 & 0 & 0 & E_{imp} & 0 & 0 & 0 & 0 \\
0 & 0 & V(x) & 0 & 0 & 0 & 0 & 0 & E_{imp} & 0 & 0 & 0 \\
0 & 0 & 0 & V(x) & 0 & 0 & 0 & 0 & 0 & E_{imp} & 0 & 0 \\
0 & 0 & 0 & 0 & V(x) & 0 & 0 & 0 & 0 & 0 & E_{imp\text{-}so} & 0 \\
0 & 0 & 0 & 0 & 0 & V(x) & 0 & 0 & 0 & 0 & 0 & E_{imp\text{-}so}
\end{vmatrix}. \quad (1)$$

The individual parameters in Eqs. (2a)–(2f) are those of the original 6×6 valence-band matrix modified by the addition of the terms $\Delta E_{VBM}x$ to H and L and $\Delta E_{SO}x$ to S, which take into account the linear change in the valence-band maximum and spin-orbit split-off band energies, respectively, between the two endpoint compounds as described by the virtual crystal approximation (VCA). Here ΔE_{VBM} and ΔE_{SO} are the total differences in valence-band maximum and spin-orbit split-off band energies between the endpoint compounds,

$$H = -\frac{\hbar^2}{2m_0}[(k_x^2 + k_y^2)(\gamma_1 + \gamma_2) + k_z^2(\gamma_1 - 2\gamma_2)] + \Delta E_{VBM}x, \quad (2a)$$

$$L = -\frac{\hbar^2}{2m_0}[(k_x^2 + k_y^2)(\gamma_1 - \gamma_2) + k_z^2(\gamma_1 + 2\gamma_2)] + \Delta E_{VBM}x, \quad (2b)$$

$$\alpha = \sqrt{3}\frac{\hbar^2}{m_0}[k_z(k_x - ik_y)\gamma_3], \quad (2c)$$

$$\beta = \frac{\sqrt{3}}{2}\frac{\hbar^2}{m_0}[(k_x^2 - k_y^2)\gamma_2 - 2ik_xk_y\gamma_3], \quad (2d)$$

$$D = L - H, \quad (2e)$$

$$S = \frac{1}{2}(L + H) - \Delta_0 - \Delta E_{SO}x. \quad (2f)$$

The Luttinger parameters and spin-orbit splitting energy were set to the corresponding values of GaAs, $\gamma_1=6.9$, $\gamma_2=2.2$, $\gamma_3=2.9$, and $\Delta_0=0.341$ eV. However, it should be noted that at the Γ point where $\mathbf{k}=0$, the off-diagonal elements of this 6×6 portion of the matrix will be zero. The term V represents the hybridization energy between the three p-like wave functions of the T_d point group of the GaAs valence bands and the counterparts of the p-like localized impurity states and is given as

$$V = \langle P_X^A|U|X\rangle = \langle P_Y^A|U|Y\rangle = \langle P_Z^A|U|Z\rangle, \quad (3)$$

where U is the localized potential of the minority species (Sb, Bi) in the GaAs crystal lattice, P^A denotes the wave function of impurity A (Sb, Bi), and X, Y, and Z refer to the Bloch wave functions of the host. Configurational averaging over the randomly distributed minority species with the fraction x yields

$$V = C_A\sqrt{x}. \quad (4)$$

The positions of the heavy/light hole levels of the impurity atoms are denoted by E_{Imp}, while $E_{Imp\text{-}so}$ refers to the corresponding spin-orbit split-off level determined from the atomic spin-orbit splitting energy. Here, the atomic spin-orbit splitting energies for Sb and Bi are assumed to be 0.6 eV and 1.5 eV, respectively.[21] Diagonalization of the matrix in Eq. (1) yields six doubly degenerate eigenvalues representing the restructured valence bands, as three distinct anticrossing in-

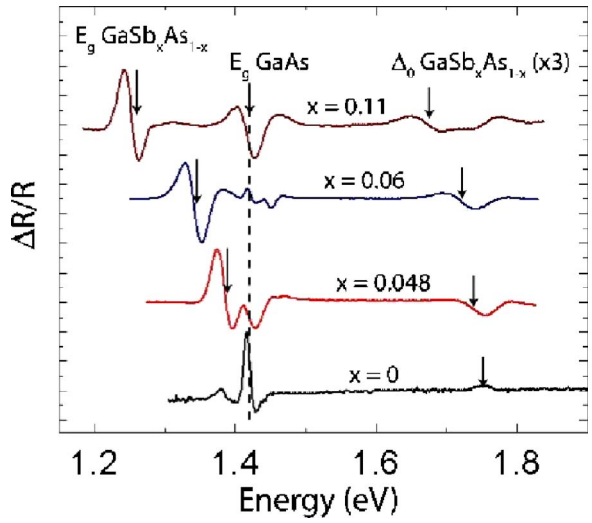

FIG. 1. (Color online) Photomodulated reflectance spectra of several $GaSb_xAs_{1-x}$ films. The dashed line is a guide to denote the composition-independent transition associated with the band gap of the GaAs substrate, while the arrows indicate the band gap and spin-orbit split-off band to conduction-band transitions of the $GaSb_xAs_{1-x}$ films

teractions are expected to produce E_- and E_+ bands of heavy hole, light hole, and spin-orbit split-off character at the Γ point. Strain effects as well as any influence of the conduction band on the restructuring of the valence band were ignored for these calculations. Finally, it should be emphasized that this model is only appropriate for describing the behavior for alloys with dilute impurity concentrations and is not meaningful once the Sb/Bi-rich phase begins to dominate the properties of the alloy.

III. VALENCE-BAND STRUCTURE OF $GaSb_xAs_{1-x}$

In order to experimentally investigate the restructuring of the valence band due to the anticrossing interactions, the room-temperature interband transition energies of several $GaSb_xAs_{1-x}$ films of various compositions were measured by photomodulated reflectance (PR) spectroscopy. The $GaSb_xAs_{1-x}$ samples used in this study were epitaxial films grown by organometallic vapor-phase epitaxy (OMVPE) and molecular beam epitaxy (MBE) with compositions of $x < 0.11$. The films were pseudomorphically grown on nominally exact (001) GaAs substrates, and the alloy compositions were determined from x-ray diffraction and Rutherford backscattering spectrometry. The probe beam consisted of monochromatic light dispersed from a tungsten lamp, while the 325 nm line of a chopped HeCd laser provided the modulation. The PR signal was detected by a Si photodiode using a phase-sensitive lock-in system. Typical PR spectra for a few selected alloy compositions are shown in Fig 1. The observed features are associated with interband optical transitions at critical points in the electronic-band structure. The energies and the line widths of the transitions were determined by fitting the PR spectra to the Aspnes third-derivative functional form.[22] The composition-independent transition at

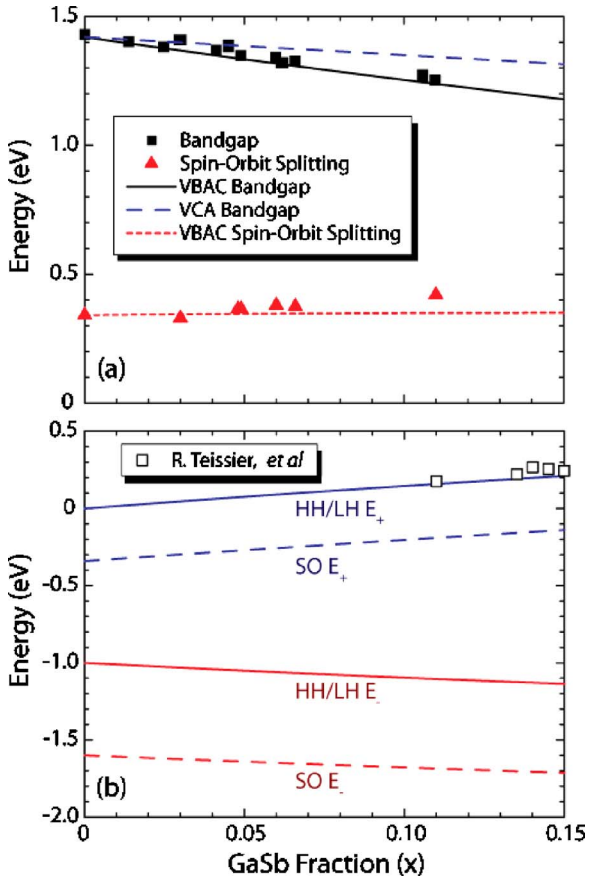

FIG. 2. (Color online) (a) Theoretically calculated band gap and spin-orbit splitting energies of $GaSb_xAs_{1-x}$, as well as the corresponding values determined experimentally by photomodulated reflectance; (b) energy positions of the heavy hole, light hole, and spin-orbit split-off E_+ and E_- bands of $GaSb_xAs_{1-x}$ as a function of GaSb fraction. Experimental values of the valence-band edge were taken from Teissier *et al.*[6]

1.42 eV is associated with the band gap of the GaAs substrate, whereas the lower energy features originate from the fundamental band gap transitions in the $GaSb_xAs_{1-x}$ film. Finally, the weak features around 1.77 eV correspond to the transitions from the spin-orbit split-off bands to the conduction bands of the film and the substrate.

In order to explain the composition dependence of the observed transition energies, we applied the VBAC model with the energy of the localized Sb level, E_{Sb}, as well as the value of the coupling parameter, C_{Sb}, as fitting parameters. In our calculations we adopted a well-established type-I band alignment between GaAs and GaSb, with conduction, valence, and spin-orbit split-off band offsets of −0.1 eV, 0.5 eV, and 0.09 eV, respectively.[23] Excellent agreement between the experimentally observed composition dependence of the band gap and spin-orbit splitting energies and the model, shown in Fig. 2(a) was obtained with E_{Sb} located 1.0 eV below the valence-band maximum (VBM) of GaAs and a C_{Sb} of 1.05 eV. Using the known atomic spin-orbit splitting energy for Sb, $E_{Sb\text{-}so}$ was positioned 1.6 eV below the VBM of GaAs. Here, the theoretical band gap is defined as the difference in energy between the VBAC valence-band

maximum and the VCA conduction-band minimum, $E_{CB\text{-}VCA}$, which can be written as

$$E_{CB\text{-}VCA} = E_g - \Delta E_{CBM} x, \tag{5}$$

where E_g is the band gap of GaAs and $\Delta E_{CBM}=0.1$ eV is the conduction-band edge offset between GaAs and GaSb.

The calculated energy levels of the $GaSb_xAs_{1-x}$ valence bands at the Γ point as functions of composition are displayed in Fig 2(b). Note the distinct upward movement of the heavy and light hole-related E_+ bands by approximately 16 meV per $x=0.01$, with a downward movement of the corresponding E_- bands. This upward shift of the heavy and light hole E_+ band edge resulting from the anticrossing interaction accounts for the majority of the band gap reduction observed As-rich in $GaSb_xAs_{1-x}$. This unusually large contribution of the valence-band shift to the band gap bowing is in good agreement with results of Teissier *et al.*, who reported that the band gap reduction in this alloy is almost completely associated with an upward movement of the valence-band edge.[6] Their experimental results demonstrating an increase in the valence-band offset between GaAs and As-rich $GaSb_xAs_{1-x}$, included in Fig. 2(b), are in close agreement with our predictions. Repulsion also occurs between the spin-orbit split-off-related E_+ and E_- bands; however, the intensity of the interaction is reduced due to the large separation between these coupled bands, and the spin-orbit E_+ band moves upward by 13 meV per $x=0.01$. As a result, the spin-orbit splitting energy increases slightly.

Using these results, the band gap bowing across the entire composition range of $GaSb_xAs_{1-x}$ may be calculated. While valence-band anticrossing interactions are primarily responsible for the band gap reduction observed for As-rich compositions, it has been demonstrated that the reduction of the band gap at Sb-rich compositions has been well explained by the corollary conduction-band anticrossing (CBAC) model.[11] In the later case, the band gap is defined as the difference between the CBAC conduction-band minimum and the VCA valence-band maximum. The overall band gap can then be determined from a weighted average of the band gaps $E_g^{\text{As-}rich}$ and $E_g^{\text{Sb-}rich}$ calculated by the valence and conduction band anticrossing models, respectively,

$$E_g(x) = (1-x)E_g^{\text{As-}rich} + xE_g^{\text{Sb-}rich}.$$

The resulting band gap trend, displayed in Fig. 3, demonstrates the significant band gap bowing. While this trend can also be fit with a single bowing parameter ($b=1.2$ eV), the quadratic relationship does not provide any substantive insight into the underlying physical mechanisms that drive the deviation from the VCA in the first place. The attractive characteristic of the band anticrossing models is that they describe the alloy composition dependence of not only the changes in the band gap but also the shifts in the band offsets and the dispersion relations for the conduction and the valence bands. This knowledge is essential for a proper description of the density of electronic states as well as optical and transport phenomena in the alloys.[11]

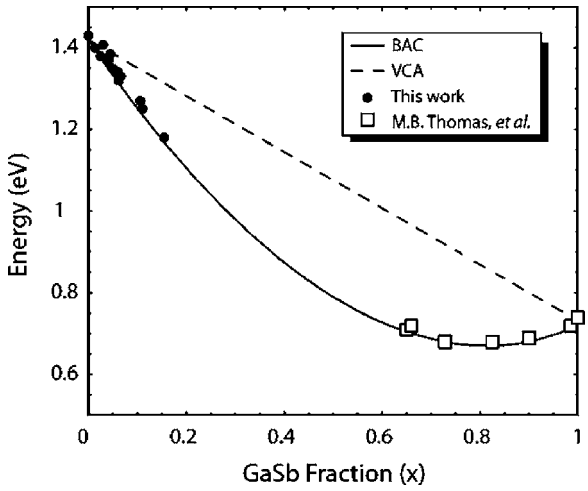

FIG. 3. Band gap of $GaSb_xAs_{1-x}$ over the full composition range. Theoretical values were calculated with a weighted average of the valence- and conduction-band anticrossing models. The experimental values at low x were determined by photomodulated reflectance, and those at high x were previously reported by Wu *et al.* (Ref. 11) and Thomas *et al.* (Ref. 28).

IV. VALENCE-BAND STRUCTURE OF $GaBi_xAs_{1-x}$

A more dramatic valence-band anticrossing interaction is expected to occur in III-Bi_x-V_{1-x} alloys in which the very large, metallic element Bi partially replaces other group V elements. $GaBi_xAs_{1-x}$ is the most extensively studied of such alloys, with Bi concentrations up to $x=0.04$ reported in the literature.[1–5] Optical studies of GaP doped with small Bi concentrations have led to the determination of the energy of the localized Bi level, E_{Bi}, which is located about 0.1 eV above the valence-band edge of GaP.[24] Assuming constancy of the localized levels relative to the vacuum level and using a valence-band offset of 0.5 eV between GaAs and GaP, we estimate that E_{Bi} and $E_{\text{Bi-}so}$ lie 0.4 eV and 1.9 eV below the VBM of GaAs, respectively. The proximity of E_{Bi} to the GaAs heavy- and light-hole bands is expected to lead to a strong anticrossing interaction between these two sets of states. However, because GaBi has never been synthesized, there is no experimental data on the band offsets between GaAs and GaBi. In order to include the VCA contributions, we have estimated the band offsets using the theoretically calculated GaBi band gap energy of -1.45 eV.[25] The valence-band offset, $\Delta E_{VBM}=0.8$ eV, was estimated from the dependence of the valence-band edge energies versus lattice constant in Ga-containing group III-V binaries. The conduction-band offset, $\Delta E_{CBM}=-2.1$ eV, was then obtained from these two values. Finally, the spin-orbit split-off band offset, $\Delta E_{SO}=-1.1$ eV, was established using the theoretically determined value of the GaBi spin-orbit splitting energy of 2.2 eV.[26]

The calculated energy gap along with experimental results reported by Francoeur *et al.*,[3] Tixier *et al.*,[4] and Huang *et al.*[5] are displayed in Fig. 4(a). The best fit to the data was obtained using a single fitting parameter, C_{Bi}, of 1.55 eV. The corresponding-band edge positions as a function of Bi concentration are shown in Fig. 4(b). Again, the band gap bow-

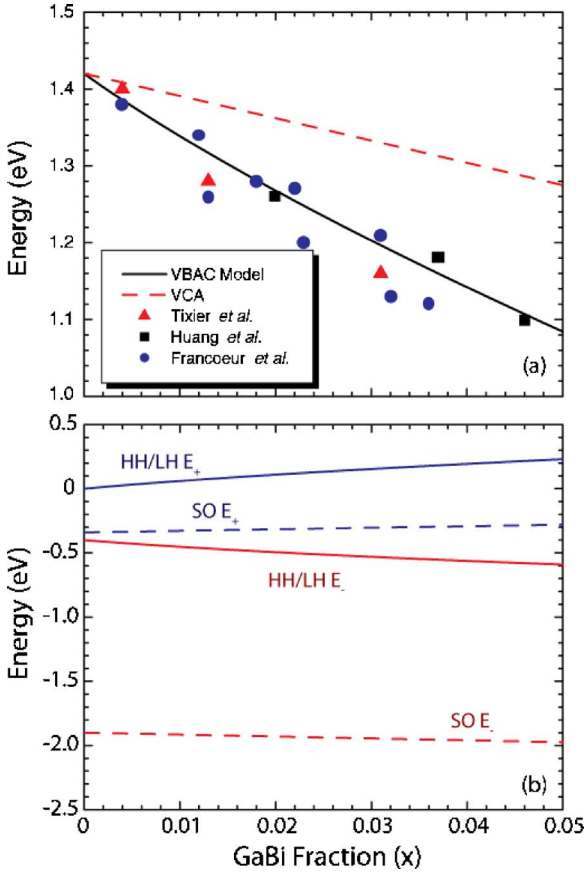

FIG. 4. (Color online) (a) $GaBi_xAs_{1-x}$ band gap as well as experimentally determined values (Refs. 3–5), (b) position of the E_+ and E_- related heavy, light, and spin-orbit split-off bands determined by the VBAC model as a function of Bi concentration.

ing observed in $GaBi_xAs_{1-x}$ is due to an upward movement of the heavy- and light-hole E_+ bands. The increase of the band gap bowing observed in $GaBi_xAs_{1-x}$ as compared to $GaSb_xAs_{1-x}$ is due to the large mismatch in ionization energies between the two anion elements as well as the close proximity of the coupled light- and heavy-hole bands.

While $GaBi_xAs_{1-x}$ has a greater lattice constant than GaAs, the addition of N can be used to lattice match the two.[25] Not only does the presence of N reduce the strain of these films grown on GaAs substrates,[5,27] but as shown by Shan *et al.*, it also further reduces the band gap through a downward shift in the conduction-band edge.[12] Thus, the positions of the conduction- and valence-band edges may be independently manipulated through careful control of the Bi and N concentrations.

V. VALENCE-BAND ANTICROSSING IN OTHER III-V SEMICONDUCTORS

At present, limited research on other dilute III-(Sb, Bi)-V materials has been reported. However, by extrapolating the parameters used to model the Ga-(Sb,Bi)-As alloys, the properties of additional systems may be inferred. Figure 5 depicts the positions of the Sb and Bi levels relative to the valence- and conduction-band edges for a variety of III-V

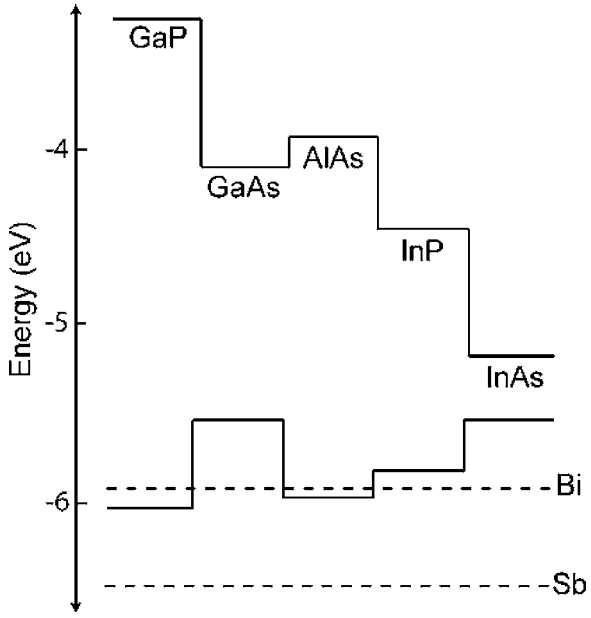

FIG. 5. Bi and Sb impurity level positions with respect to the conduction and valence bands of various III-V semiconductors. The energy scale is relative to the vacuum level (Ref. 23).

semiconductors at the Γ point, which may be used as a guide to determine the importance of the anticrossing interactions within the valence band. For example, the Sb and Bi impurity levels lie below the valence-band maximum of InAs and InP, and band gap bowing is expected to occur via an upward shift of valence-band edge in In-(Sb,Bi)-As and In-(Sb,Bi)-P alloys as well. Alternatively, a multiband semiconductor may be formed through the addition of Bi if the impurity level is located within the band gap of the host material. Such is the case with $GaBi_xP_{1-x}$, and $AlBi_xAs_{1-x}$ alloys where the Bi level is positioned above the valence-band maximum of GaP and AlAs, respectively. Anticrossing interactions are predicted to push the Bi-derived heavy- and light-hole E_+ bands into the band gap of these semiconductors, creating a narrow impurity-related band. This is analogous to the case of N-rich $GaAs_xN_{1-x}$, in which a narrow As-related band develops well above the valence-band edge.[17]

In order to model the $GaBi_xP_{1-x}$ alloy system, we have used the general trend in ionization energy vs coupling parameter observed in $GaSb_xAs_{1-x}$ and $GaBi_xAs_{1-x}$ to set C_{Bi} at 2.1 eV. Conduction, valence, and spin-orbit split-off band offsets between GaP and GaBi were determined in a similar manner to those in the $GaBi_xAs_{1-x}$ system and were set to −3.03 eV, 1.2 eV, and −0.92 eV, respectively. The resulting valence-band edge energies as a function of Bi content are shown in Fig. 6. The initial decrease in the position of the heavy- and light-hole E_- levels as a function of x is a result of the anticrossing interaction with the heavy- and light-hole E_+ levels, while the subsequent rise is due to a secondary anticrossing interaction with the spin-orbit split-off E_+ band. Of particular note is the drastic rise in the location of the heavy- and light-hole E_+ bands, which shift upward by approximately 0.1 eV for x=0.01. From these predictions, a very large gap reduction is expected in $GaBi_xP_{1-x}$ alloys along with a large enhancement of the spin-orbit splitting

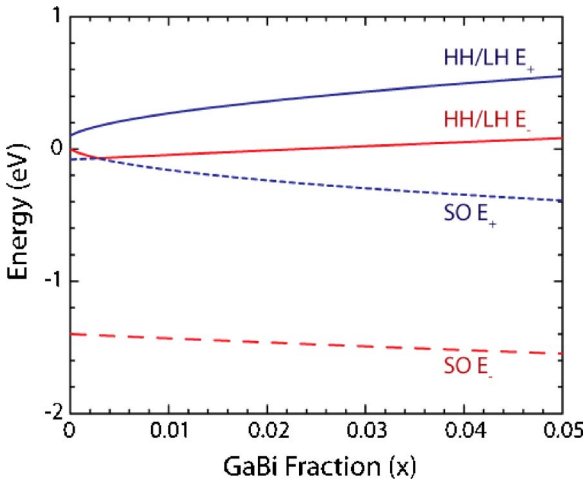

FIG. 6. (Color online) Relative positions of the E_+ and E_- valence-band edges in $GaBi_xP_{1-x}$.

energy, which reaches approximately 1 eV for $x=0.05$. Although these results are only estimates, they clearly indicate that through judicious adjustment of the alloy composition the electronic structure of the valence band of $GaBi_xP_{1-x}$ can be significantly modified and may be tuned to meet specific requirements of potential device applications.

VI. CONCLUSIONS

In summary, the band gap bowing observed in $GaSb_xAs_{1-x}$ and $GaBi_xAs_{1-x}$ is well explained by the valence-band anticrossing model. The addition of a few atomic percent of Sb or Bi to GaAs results in a restructuring of the valence band, and the upward movement of the heavy- and light-hole E_+ bands leads to a reduction of the band gap. This model can be readily applied to the investigation of other III-(Sb,B)-V systems.

ACKNOWLEDGMENTS

This work is supported by the director, Office of Science, Office of Basic Energy Sciences, Division of Materials Sciences and Engineering, of the U.S. Department of Energy under Contract No. DE-AC02-05CH11231. KA acknowledges support from NSF-IGERT.

[1] K. Oe and H. Okamoto, Jpn. J. Appl. Phys., Part 2 **37**, L1283 (1998).
[2] J. Yoshida, T. Kita, O. Wada, and K. Oe, Jpn. J. Appl. Phys., Part 1 **42**, 371 (2003).
[3] S. Francoeur, M. J. Seong, A. Mascarenhas, S. Tixier, M. Adamcyk, and T. Tiedje, Appl. Phys. Lett. **82**, 3874 (2003).
[4] S. Tixier, M. Adamcyk, T. Tiedje, S. Francoeur, A. Mascarenhas, P. Wei, and F. Schiettekatte, Appl. Phys. Lett. **82**, 2245 (2003).
[5] W. Huang, K. Oe, G. Feng, and M. Yoshimoto, J. Appl. Phys. **98**, 053505 (2005).
[6] R. Teissier, D. Sicault, J. C. Harmand, G. Ungaro, G. Le Roux, and L. Largeau, J. Appl. Phys. **89**, 5473 (2001).
[7] R. E. Nahory, M. A. Pollack, J. C. DeWinter, and K. M. Williams, J. Appl. Phys. **48**, 1607 (1977).
[8] J. L. Castano and J. Piqueras, J. Appl. Phys. **54**, 3422 (1983).
[9] R. M. Cohen, M. J. Cherng, R. E. Benner, and G. B. Stringfellow, J. Appl. Phys. **57**, 4817 (1985).
[10] B. Fluegel, S. Francoeur, A. Mascarenhas, S. Tixier, E. C. Young, and T. Tiedje, Phys. Rev. Lett. **97**, 067205 (2006).
[11] J. Wu, W. Shan, and W. Walukiewicz, Semicond. Sci. Technol. **17**, 860 (2002).
[12] W. Shan, W. Walukiewicz, J. W. Ager III, E. E. Haller, J. F. Geisz, D. J. Friedman, J. M. Olson, and S. R. Kurtz, Phys. Rev. Lett. **82**, 1221 (1999).
[13] K. M. Yu, W. Walukiewicz, J. Wu, W. Shan, J. W. Beeman, M. A. Scarpulla, O. D. Dubon, and P. Becla, Phys. Rev. Lett. **91**, 246403 (2003).
[14] M. Weyers, M. Sato, and H. Ando, Jpn. J. Appl. Phys., Part 2 **31**, L853 (1992).
[15] C. Skierbiszewski, Appl. Phys. Lett. **76**, 2409 (2000).
[16] W. Shan, W. Walukiewicz, J. Wu, K. M. Yu, J. W. Ager III, S. X. Li, E. E. Haller, J. F. Geisz, D. J. Friedman, and S. R. Kurtz, J. Appl. Phys. **93**, 2696 (2003).
[17] J. Wu, W. Walukiewicz, K. M. Yu, J. D. Denlinger, W. Shan, J. W. Ager III, A. Kimura, H. F. Tang, and T. F. Kuech, Phys. Rev. B **70**, 115214 (2004).
[18] J. Wu, W. Walukiewicz, K. M. Yu, E. E. Haller, I. Miotkowski, A. K. Ramdas, Ching-Hau Su, I. K. Sou, R. C. C. Perera, and J. D. Denlinger, Phys. Rev. B **67**, 035207 (2003).
[19] R. People and S. K. Sputz, Phys. Rev. B **41**, 8431 (1990).
[20] M. A. Ivanov and Yu. G. Pogorelov, Sov. Phys. JETP **49**, 510 (1979); M. A. Ivanov and Yu. G. Pogorelov, *ibid.* **61**, 1033 (1985).
[21] X. Gonze, J.-P. Michenaud, and J.-P. Vigneron, Phys. Rev. B **41**, 11827 (1990).
[22] D. E. Aspnes, Surf. Sci. **37**, 418 (1973).
[23] S. Tiwari and D. J. Frank, Appl. Phys. Lett. **60**, 630 (1992).
[24] F. A. Trumbore, M. Gershenzon, and D. G. Thomas, Appl. Phys. Lett. **9**, 4 (1966).
[25] A. Janotti, S. H. Wei, and S. B. Zhang, Phys. Rev. B **65**, 115203 (2002).
[26] Y. Zhang, A. Mascarenhas, and L.-W. Wang, Phys. Rev. B **71**, 155201 (2005).
[27] S. Tixier, S. E. Webster, E. C. Young, T. Tiedje, S. Francoeur, A. Mascarenhas, P. Wei, and F. Schiettekatte, Appl. Phys. Lett. **86**, 112113 (2005).
[28] M. B. Thomas, W. M. Coderre, and J. Wooley, Phys. Status Solidi A **2**, K141 (1970).